Nancy R. Sottos[1], David L. Hiemstra[2] and William R. Scott[3]

CORRELATING INTERPHASE GLASS TRANSITION AND INTERFACIAL MICROCRACKING IN POLYMER COMPOSITES

REFERENCE: Sottos, N.R., Hiemstra, D.L. and Scott, W.R., "Correlating Interphase Glass Transition and Interfacial Microcracking in Polymer Composites," Fracture Mechanics: 25th Volume, ASTM STP 1220, F. Erdogan and Ronald J. Hartranft, Eds., American Society for Testing and Materials, Philadelphia, 1994.

ABSTRACT: The glass transition temperature of the interphase was tailored to investigate its influence on micromechanical behavior. Three different types of experiments were carried out on the samples with tailored interphases. First, interferometric measurements were made on samples consisting of a single 30 micron carbon fiber coated with a low T_g resin and embedded in an epoxy matrix. The resulting displacement profiles were compared with those of an uncoated fiber. Second, single fiber fragmentation tests were performed over a range of temperatures for samples consisting of 7 micron AS4 carbon fibers which were either coated with the same low T_g resin, a higher T_g resin or left uncoated. Finally, microcracking investigations were performed by subjecting a cluster of four fibers with tailored interphases to various thermal loads. The location and occurrence of microcracking were correlated with interphase T_g. Both the interferometric results and the single fiber fragmentation results supported the existence of an interphase with reduced glass transition temperature in uncoated samples. Interphase glass transition temperature had a significant effect on both load transfer and thermally induced microcracking observed in the experiments. Additionally, it was shown that the interphase can be tailored to either enhance or hinder the observed effects.

KEYWORDS: fiber/matrix interface, interphase glass transition, micro-interferometry interfacial shear strength, interfacial microcracking

---

INTRODUCTION

The existence, properties and influence of an interphase region have been the subject of much research in advanced composite materials. In general, the interphase in a polymer matrix composite can be formed by three basic mechanisms: chemical bonding, molecular

---

[1] Assistant Professor, Department of Theoretical and Applied Mechanics, University of Illinois, Urbana, IL 61801

[2] Development Engineer, Prince Corporation, One Prince Center, Holland, MI 49423

[3] Group Leader, Naval Air Warfare Center, Aircraft Division, Code 6063, Warminster, PA 18974

segregation, and van der Waal bonding [1]. Through these mechanisms, structural gradients may be created in the matrix due to the influence of the fiber surface on the natural configurations of the polymer chains. Any variations in matrix structure and chemistry near the fiber surface cause gradients in the material properties of that region.

Several researchers have found evidence that structural gradients in a polymer matrix lead to an altered glass transition temperature. Pogany [2] first showed that non-stoichiometric concentrations of an aliphatic polyamine crosslinked with an epoxy resin caused reductions in the glass transition temperature. Lipatov, et al. [3] concluded a selective sorption of one of the components in a filled epoxy system occured on the filler surface before hardening. A surplus of the other component acted as a plasticizer which caused a reduction of elastic modulus and a change in the relaxation behavior of the filled system. Crowson and Arridge[4] provided evidence for a difference in glass transition temperature between filled and unfilled epoxy systems. Additionally, Papanicolaou, et al. [5] discussed the concept of the existence of a viscoelastic interphase with a lower glass transition temperature.

Palmese and McCullough [6] measured changes in glass transition temperature as a function amine concentration for the EPON 828/PACM system using both dynamic and thermal mechanical analysis (DMA and TMA). At the stoichiometric point of this resin (28 parts PACM to 100 parts EPON 828), the glass transition temperature is 160°C. For amine concentrations both above and below the stoichiometric point, the value of T_g is significantly reduced. If the fiber surface alters the cure chemistry such that a non-stoichiometric mixture of amine and epoxy occurs, the material in that region would in theory have a much lower glass transition temperature than the neat resin.

Recent interferometric investigations by Sottos, et al. [7] presented in-situ experimental evidence for the existence of an interphase region with a glass transition temperature that is significantly lower than that of the neat resin. Thermal displacements were measured using a scanning micro-interferometer for samples consisting of a single carbon fiber embedded in an epoxy matrix. Comparison of experimental profiles measured by the interferometer with theoretical displacement predictions indicated that the value of the matrix properties near the fiber surface differed appreciably from the value in the neat resin. The difference between the experimental and theoretical curves when no interphase was considered was too large to be accounted for by experimental error or small variations in the properties of the matrix. A thin interphase region of 0.06 fiber radii, with a modulus two orders of magnitude lower than the neat resin, most closely matched the experimental profiles. In order for the modulus to be this low, the epoxy in this region would have to be heated to a temperature above its glass transition.

The existence of a reduced glass transition temperature has significant implications for the thermal behavior and long term performance of a composite. If the interphase had a lower glass transition temperature, the region would have a pronounced effect on the fracture toughness, durability and local stress state of the composite. Such a low modulus region would act to arrest crack growth in the matrix and significantly increase the fracture toughness. On the other hand, the performance of the composite would be significantly reduced at high temperatures. Consequently, the interphase has the potential to be tailored to enhance or hinder these effects depending on the application.

In the current investigation, the glass transition temperature of the interphase was tailored to investigate its influence on micromechanical behavior. Three different types of experi-ments were carried out on samples with tailored interphases. First, interferometric measurements were made on samples consisting of a single 30 micron carbon fiber coated with a low T_g resin and embedded in an epoxy matrix. The resulting

displace-ment profiles were compared with those of an uncoated fiber. Second, single fiber fragmentation tests were performed over a range of temperatures for samples consisting of 7 micron AS4 carbon fibers which were either coated with the same low T_g resin, a higher T_g resin or left uncoated. Finally, microcracking investigations were performed by subjecting a cluster of four fibers with tailored interphases to various thermal loads. Optical and scanning electron microscopy were utilized to study the location and occurrence of microcracking which were then correlated with interphase T_g.

TAILORING INTERPHASE PROPERTIES

In order to study the influence of glass transition temperature on micromechanical behavior, three different experiments (discussed in subsequent sections) were performed on samples with tailored interphases. Three different types of interphases were investigated: low modulus/low glass transition temperature, higher modulus/higher glass transition temperature, and uncoated. In each experiment, fibers were either coated with a resin of known Tg or left uncoated and then embedded in an epoxy matrix. Shell EPON 828 (diglycidyl ether of bisphenol A*) resin cured with AMICURE PACM [bis(p-amino cyclohexyl) methane] was chosen for the matrix material.

Samples with three different interphases were prepared as follows. All fibers were washed in isopropyl alcohol to remove any surface lubricants or contaminants and allowed to dry. In the first type of sample (type I), the fibers were left uncoated . For the second type of sample (type II), fibers were coated with a thin layer of EPON 871 resin to reduce the glass transition and modulus of the interphase. EPON 871 (aliphatic polyepoxide) is an amber, low viscosity liquid which imparts increased flexibility to EPON 828 compositions. The fibers were coated by gently pulling single filaments through a bath of the resin. For the third type of sample (type III), fibers were coated with a thin layer of a stoichiometric mix of EPON Resin DPS-164 (Epoxy cresol novolac) and PACM. An interphase with a glass transition temperature of 150°C and slightly higher modulus was obtained. The solid DPS 164 was first dissolved in acetone, then mixed with PACM. After evaporating the acetone, the coating was cured on the fibers. The Young's modulus measured by room temperature tensile tests and glass transition temperature measured by DSC (Differential Scanning Calorimetry) for the matrix and coatings are listed in Table 1.

Table 1. Properties of Matrix and Coatings

Resin	E (GPa)	T_g (°C)
Neat Matrix - (EPON 828 + PACM)	2.5	160
Coating II -(EPON 871 +828 + PACM)	2.1	80
Coating III - (EPON DPS 164 + PACM)	3.5	150

MICRO-INTERFEROMETRIC MEASUREMENTS

Micro-interferometry was utilized to study differences in the thermal displacements caused by changing the interphase glass transition temperature. Previous interferometric work by Sottos, et al [7], presented evidence for the existence of an interphase region associated with untreated fibers (no coating) with a lower glass transition temperature than the neat resin. Hence, the thermal displacement behavior observed for untreated fibers should be enhanced by coating the fibers with a low T_g resin.

A detailed description of the interferometric experimental technique utilized for the displacement measurements is given by Sottos, et al. [8,9] and Ryan, et al. [10]. A single, linearly polarized light beam from an Argon laser is incident upon a 40 MHz acousto-optic modulator (AOM) producing two beams which are sent along different arms of the interferometer. The first beam (reference beam) propagates with the same frequency as the beam incident upon the AOM. The second beam is shifted in frequency by 40 MHz and is used to illuminate the sample surface. The two beams are recombined in a beam splitter and then arrive at the primary lens of a long distance microscope. An image is formed behind the microscope and is magnified onto the image plane of a scanning photodiode detector using an eyepiece lens. The light that forms the sample image differs in frequency by 40 MHz from the light that forms the reference image. Thus, any z-axis displacement of the sample surface will produce phase shifts in the 40 MHz beat signal arriving at the photodetector. A lock-in amplifier is used to compare the phase of the 40 MHz signals from both the reference and the scanning detectors. This technique has the capability of measuring thermal displacements with an out-of-plane resolution of 50 angstroms and a possible in-plane resolution of 0.5 microns.

Experimental Procedure

Interferometric measurements of thermal displacements were made on type I (uncoated) and type II (low T_g) samples only. Specimens were prepared by placing a single carbon fiber, coated or uncoated, into the center of a mold which was then filled with a stoichio-metric mix of EPON 828 and PACM. A schematic of the sample is shown in Fig. 1.

The fibers used for the interferometric studies were untreated 30 micron pitch base carbon fibers supplied by Textron Specialty Materials. The longitudinal Young's modulus of these fibers was specified by the manufacturer as E_L=41.0 MPa. Values for the longitudinal thermal expansion coefficient, α= -0.5 x10^{-6} °C^{-1}, thermal conductivity, K= 8.3 W/m °C, and Poisson's ratio, ν_{LT}=0.22, were taken from the literature [11].

All samples were held for 1 hour at 80°C to minimize the bubbles in the resin phase, then cured for 1 hour at 150°C, and allowed to slow cool to room temperature overnight. The EPON 871 coating (type II samples) applied to the fibers was approximately 5.0 microns thick. Because the 871 mixes and reacts with the EPON 828/PACM matrix, it is difficult to determine the exact width of the interphase after curing.

Specimens were cut to a length of approximately 2 cm and the front and back faces were polished metallographically. Polishing of the front face on which the measurements were made was critical to insure a specularly reflective surface. The radius of the fibers was determined to be exactly 17.2 microns from a photomicrograph of the sample surfaces. The outer radius of the samples measured 15.88 mm.

Samples were heated by passing a small current of 10.0 mA through the fiber. Leads were attached to both the front and back polished faces of the specimen as shown in Fig. 1. A thin layer of gold was sputtered onto the surface to provide both a current conduction path and a highly reflective surface across the circular cross-section of the fiber/matrix interface. There were several advantages to heating the sample electrically in this manner. A repeatable, radial temperature field was generated in the sample which could be predicted analytically. The equilibrium time for heating and cooling the region of interest was small (typically less than ten seconds). Finally, there was minimal convection of heat into the interferometer path minimizing thermal effects on the apparatus.

Analytical prediction of the temperature distribution in the sample required the solution of the heat conduction equation for an electrically heated fiber embedded in an epoxy matrix. This problem has been solved previously by Sottos, et al.[9] and was used to calculate the steady state temperature field. As a result of applying 58 mW of power to the samples, the temperature in the fiber was predicted to be nearly constant at 60°C, while the matrix temperature was found to decrease rapidly away from the interface. The analytical prediction for fiber temperature was compared with experimental values and found to differ by less than five percent.

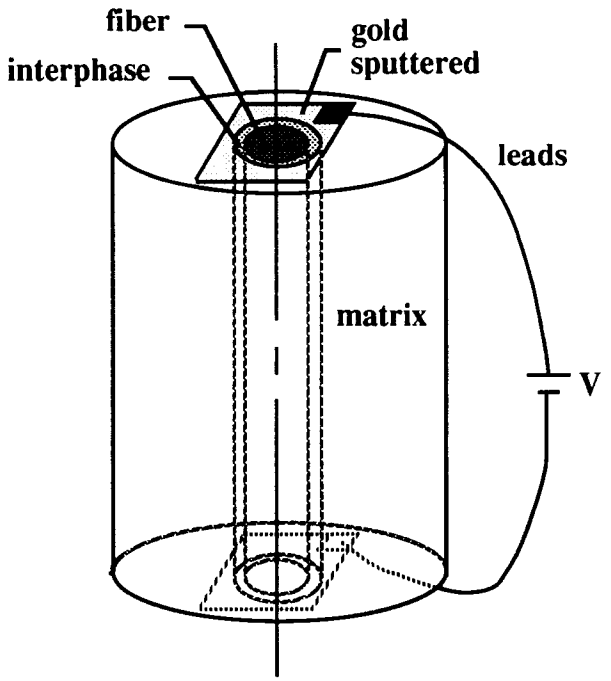

Fig. 1 Schematic of single fiber interferometric sample.

Displacement Profiles

To measure the thermal displacements in the interphase, it was convenient to make measurements on single scan lines extending across the fiber center. The magnification of the interferometer was 25X for these measurements so that the far field matrix could be included in the scan. Heating the sample caused the matrix to expand upwardly and pull the fiber with it. Subtraction of an initial unheated scan line from the heated scan line yielded the net thermal displacement of the region.

A series of displacement measurements was made on both types of samples. All of the displacement data were normalized to account for small differences in sample height and to facilitate theoretical comparisons. Fig. 2 is a plot of the thermal displacements for both the coated and uncoated single fiber samples. The displacements are plotted as a function of radial distance with the fiber center at r=0. The displacement data were averaged for three consecutive runs on each sample and then normalized by subtracting from each point the value of the displacement of a reference point at 20 fiber radii out. The displacement across the fiber is nearly constant. However, there is a sharp rise in the displacement of the matrix near the interface, which peaks at about 5 fiber radii out. After this point, the matrix displacements decrease almost linearly with radial distance.

The gradient at the interface and consequently the displacement of the matrix are significantly larger, however, for the coated fiber. Hence, the interferometric method was capable of detecting different surface treatments or coatings applied to the fiber.

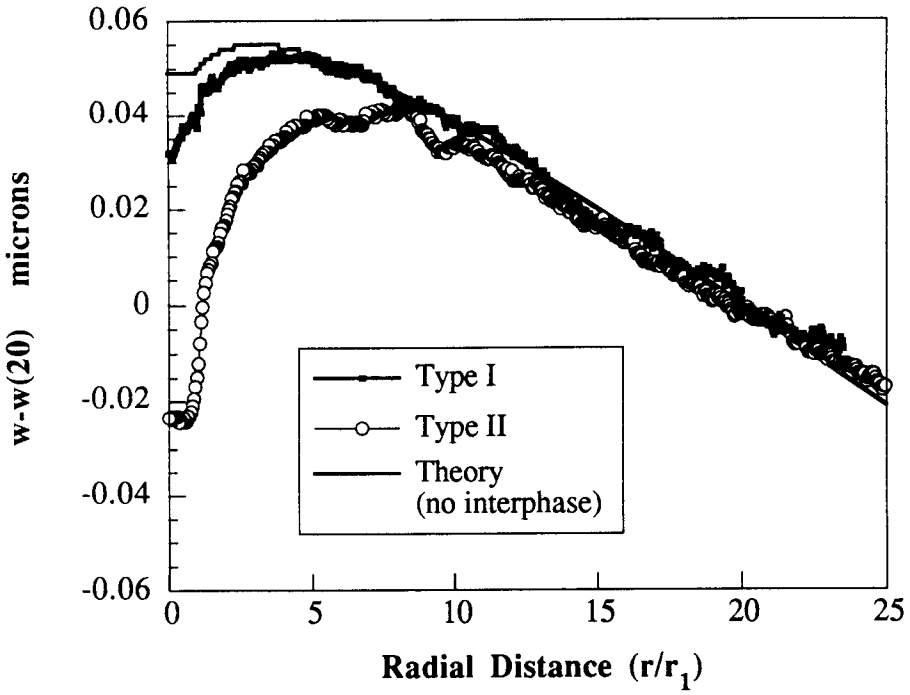

Fig. 2 Average axial displacement as a function of radial distance from the fiber center for type I and II samples compared to theoretical predictions for no interphase.

In the previous study by Sottos, et al [7], a thermal displacement solution was derived for a three phase, finite, composite cylinder model using a displacement potential approach. This linear elastic solution assumed the matrix, fiber and interphase were isotropic and yielded the following form for axial displacements [7]:

$$w^{(i)} = \sum_{n=1}^{\infty} \sin(\kappa_n z)\left[-\frac{1}{2} r m^{(i)} f_{1n} + D_{1n}^{(i)} h_{3n}^{(i)} + D_{2n}^{(i)} g_{3n}^{(i)} + D_{3n}^{(i)} h_{4n}^{(i)} + D_{4n}^{(i)} g_{4n}^{(i)}\right] \qquad (1)$$

The indices i=*1,2,3* are used to denote the fiber, interphase and matrix domains, respectively. The functions , $h_{3n}^{(i)}$, $h_{4n}^{(i)}$, $g_{3n}^{(i)}$, $g_{4n}^{(i)}$ and f_{1n}, are a combination of modified Bessel functions and can be expressed in terms of the engineering constants, E and ν, as follows:

$$
\begin{aligned}
f_{1n} &= \left[A_n I_1(\kappa_n r) - B_n K_1(\kappa_n r)\right] \\
h_{3n}^{(i)} &= \left(\frac{1+\nu^{(i)}}{E^{(i)}}\right)\kappa_n^2 I_o(\kappa_n r) \\
h_{4n}^{(i)} &= \left(\frac{1+\nu^{(i)}}{E^{(i)}}\right)\kappa_n^2\left[4(1-\nu)I_o(\kappa_n r) + \kappa_n r I_1(\kappa_n r)\right] \\
g_{3n}^{(i)} &= \left(\frac{1+\nu^{(i)}}{E^{(i)}}\right)\kappa_n^2 K_o(\kappa_n r) \\
g_{4n}^{(i)} &= \left(\frac{1+\nu^{(i)}}{E^{(i)}}\right)\kappa_n^2\left[-4(1-\nu)K_o(\kappa_n r) + \kappa_n r K_1(\kappa_n r)\right]
\end{aligned}
\tag{2}
$$

Through the use of Eq. (1), the theoretical displacements were calculated without considering the influence of an interphase and compared with the experimental results. In Fig. 2, the resulting theoretical displacement curve for no interphase is plotted along with the experimental profiles as a function of radial distance from the fiber center at r=0. The displacement values have again been normalized by subtracting the value of the displacement at 20 fiber radii out from the fiber.

For the uncoated fiber case (type I), the theoretical and experimental predictions are in excellent agreement from about 5 fiber radii out to the far field matrix. At closer than 5 fiber radii to the fiber center, the two curves start to differ dramatically. The experimental value for the fiber displacement is much less than predicted by theory for a uniform matrix with no interphase. Consequently, there is a much sharper gradient in the experimental displacement curve at the fiber/matrix interface. This result is consistent with the measurements made in previous studies [7]. When the sample is heated, the matrix material near the fiber surface does not behave as predicted for a uniform matrix with no interphase, while the matrix in the far field does behave as the neat resin.

For the coated fiber (type II), the difference between the theoretical predictions and the experimental profile is more dramatic. As discussed previously, the gradient in displacement near the fiber/matrix interface is significantly larger. Theory and experiment are only in agreement at greater than 10 fiber radii from the fiber center. Hence, the effects of the coating propagate out into the matrix further than the thickness of the coating itself.

In other studies [7,12], the experimental profiles for both types of samples were compared to displacement predictions which considered the influence of a distinct interphase region with properties significantly different from the neat matrix. Although the theoretical predictions involved many assumptions, they were sufficient to show the trends in interphase properties needed to produce the measured displacement profiles. For type I (uncoated) samples, it was shown that a modulus an order of magnitude lower than that of the neat resin most closely matched the experimental data. To obtain a modulus this low, the epoxy would have to be heated to a temperature above its glass transition. Using values of modulus and coefficient of thermal expansion measured of the EPON 828 / PACM matrix measured above T_g, an interphase width of 0.06 fiber radii was found to most closely match the experimental data. For the type II samples, a much larger interphase width of 0.6 fiber radii was necessary to match the sharp displacement profiles near the fiber/matrix interface. Overall, the enhancement of the displacement

gradient for the type II samples with a tailored low Tg interphase provides further evidence for the existence of a low Tg interphase in the untreated type I samples.

SINGLE FIBER FRAGMENTATION TESTS

In order to assess the influence of interphase modulus and glass transition temperature on the interfacial shear strength, single fiber fragmentation tests were performed over a range of temperatures on all three types of samples with tailored interphases. Temperature has been shown to have a significant effect on the interfacial shear strength predicted by single fiber fragmentation tests [13-20]. In each of these investigations, an increase in critical length was observed with increasing temperature. Several studies noted that the resulting decrease in interfacial shear strength occurred at temperatures lower than the glass transition temperature of the matrix, indicating the presence of an interphase layer with different properties [13,15,20]. The thermal stresses caused by changes in temperature also have a significant influence on the interfacial shear strength.

Experimental Procedure

Single fiber fragmentation specimens consisted of either a coated or uncoated Hercules AS4 carbon fiber (7 micron diameter approx.) embedded in dog bone coupon of an EPON 828/PACM epoxy matrix as described by Drzal, et al. [21]. Fiber coatings were approximately 1 micron thick. The specimens were then cured for 1 hour at 80°C and 1 hour at 150°C and allowed to cool to room temperature slowly to minimize residual stresses. Once fabricated, the samples were loaded in tension using a small hand operated tensile apparatus so that the fiber fractured into small pieces within the matrix. The fracture process continued until the fiber pieces reached a minimum critical length. The fiber lengths as well as the fiber diameter were then carefully measured under the microscope. Samples were tested at room temperature, 60°C, 80°C, and 100°C. Temperatures above 100°C were not considered. Heated tests were performed in a temperature controlled oven normally used for full scale mechanical testing and then examined under the microscope. Fifteen samples were tested at each temperature.

According to the elastic-plastic shear lag analysis of Kelly [22], the interfacial shear strength, τ, is inversely proportional to the critical length and is expressed as

$$\tau = \frac{\sigma_f d}{2 l_c} \tag{3}$$

where l_c is the critical length, d is the fiber diameter, and σ_f is the fiber strength. However, if many samples are tested the data can be fitted to a two parameter Weibull distribution. The mean interfacial shear strength is calculated by the relation [4]:

$$\tau = \frac{\sigma_f}{2\beta} \Gamma\left(1 - \frac{1}{\alpha}\right) \tag{4}$$

where the parameters α and β are determined by

$$\frac{\sum X_i^{\alpha}}{\ln\left(\sum X_i\right)} \sum X_i^{\alpha} - \frac{1}{\alpha} - \frac{\ln\left(\sum X_i\right)}{n} = 0 \tag{5}$$

$$\beta = \left(\frac{1}{n} \sum X_i \right)^{\frac{1}{\alpha}} \tag{6}$$

where $X_i = {}^{l_c}/_{d}$, n is the number of measurements, and Γ is the gamma function.

Test Results and Discussion

The interfacial shear strengths (IFSS) measured at room temperature for the three different types of samples are listed in Table 2. The interfacial shear strengths were calculated using Eq.(4) and a fiber strength of σ_f = 4.7 GPa. Type II (low T_g) had a slightly higher IFSS than the value measured for Type I samples (no coating), while the type III (higher T_g) samples had a lower IFSS. Overall, the addition of the coatings had only a small effect on IFSS at room temperature.

Table 2. Room Temperature IFSS

Sample Type	τ_0 (MPa)
I	44.2
II	45.2
III	40.0

The influence of temperature on the fragmentation test results is summarized in Fig. 3. IFSS is plotted as a function of temperature for all three types of samples. All values of IFSS have been normalized by the value at room temperature for each particular type of sample (τ_0). A decrease in IFSS with temperature is observed for all three samples. Heating to a moderate temperature of 60°C caused a 15% reduction in IFSS for type II (lower T_g coating) samples, a 10% reduction for type I (no coating) and no reduction in IFSS for type III (higher T_g coating) samples. At intermediate temperatures (80-85°C), the value of IFSS decreased by 22% for type II samples and 15% for type I, while the value for type III samples only decreased about 4%. Heating to 100°C caused nearly a 26% reduction in IFSS for both type I and type II samples. Only a 10% decrease in IFSS was recorded for type III samples. The reversal in curvature observed for Type II (low Tg coating) samples is consistent with the results of Wimolkiatisak and Bell [15] suggesting that the failure in these samples is more interphase/matrix dominated than interface dominated.

The observed decrease in IFSS with increasing temperature for type I and II samples is consistent with the results of previous studies [13-20]. Ohsawa, et al. [16] found the critical length of a glass fiber in epoxy resin significantly increased with temperature, causing a corresponding decrease in IFSS. The authors concluded that the decreasing values could not be explained solely by thermal stresses between the fiber and matrix and suggested that this phenomenon was brought about by a decrease in the shear strength of the matrix. The Ohsawa tests were performed in a range from 40°C - 100°C, while the glass transition temperature of the epoxy matrix was 60°C. In other investigations [13,14,20], the single fiber fragmentation tests were performed at temperatures below the T_g of the neat matrix. Reductions in IFSS were observed at temperatures far below the T_g of the neat resin where no appreciable softening of the resin should occur.

A comparison of the T_g measured for the coatings and resin listed in Table 1 with the reductions in IFSS observed in Fig. 3 provides considerable insight into the nature of interphase glass transition. Only small reductions in IFSS were measured for type III samples which had a tailored interphase with a T_g of 150°C. Large reductions in IFSS (15%) were recorded at 60° C for type II samples which had a tailored interphase with a T_g of approximately 80°C. The behavior of these two samples is somewhat expected given the relationship of their known interphase T_g in relation to the test temperature. A large drop in modulus occurs near the Tg which should lead to a reduction in load transfer, and hence IFSS. The behavior of the uncoated type I samples is less intuitive and has interesting implications. Significant reductions in IFSS where observed around 80°C, far from the glass transition temperature of the neat resin (160°C). These results also tend to support the existence of an interphase in the untreated sample, which has a reduced glass transition temperature.

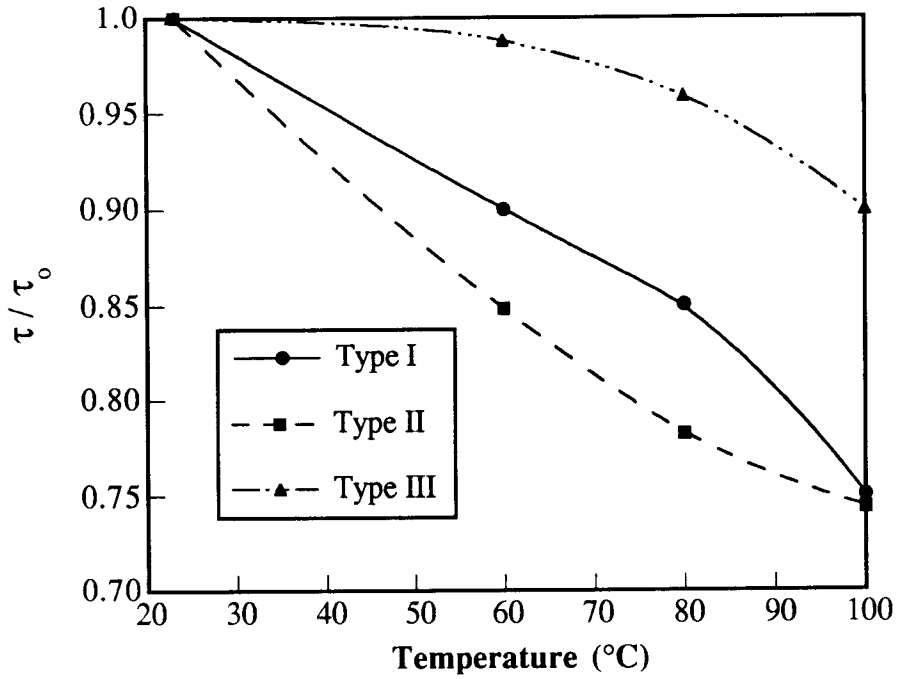

Fig. 3 Variation of normalized interfacial shear strength (τ/τ_o) with temperature for the three types of samples.

MICROCRACKING OBSERVATIONS

Significant interfacial thermal and residual stresses can develop in advanced composites because of large differences in elastic moduli and thermal expansion coefficients between the fiber and the matrix. The influence of a distinct interphase region on the local thermal stresses has also been extensively investigated [23-33]. These studies have demonstrated the significant influence of interphase material properties on the magnitude and distribution of local thermal stresses. If the elastic modulus of the interphase is lower than the value for the neat resin, local thermal stresses are reduced. Similarly, an increase in the interphase modulus leads to an increase in the magnitude of

the stresses. These micro-stresses may become large enough, even in the absence of applied loads, to cause material damage such as matrix microcracking.

Recent investigations by Hiemstra and Sottos [33] utilized both finite element analysis and experimental observations to investigate the influence of inter-fiber spacing and interphase properties on thermally induced microcracking in a cluster of fibers. Local thermal stresses were predicted as fiber spacing was systematically decreased and interphase properties were varied. Both the computational and experimental results demonstrated that interphase moduli and fiber spacing alter the location of the maximum equivalent stress and the initiation of microcracks. Because glass transition temperature influences the modulus, it should also have a significant effect on the initiation of microcracks in polymer matrix composites.

Description of Experiment

Several samples consisting of an array of four fibers with tailored interphases (types I, II and III) were subject to thermal loads high enough to initiate microcracking. In order to mount four fibers in a square array with small inter-fiber spacings, 140 micron silicon carbide fibers supplied by Textron Specialty Materials were used in place of 7 micron carbon fibers. The array of fibers was placed in the center of a mold which was then filled with a stoichiometric mix of EPON 828 resin and PACM. Prior to mounting the fibers, the thickness of each coating was measured under a microscope. The coatings had an average thickness of about 8.5 microns which was approximately 1/10 of the radius of the silicon carbide fibers. All samples were cured for 1 hour at 80°C followed by 1 hour at 150°C. The samples were then allowed to cool slowly overnight to room temperature. After curing, the samples were cut and polished metallographically. A diamond grinding wheel and diamond paste were used for polishing with a 1/4 micron diamond paste used for a final polish.

The specimens were subjected to increasing thermal loads and then observed under the microscope to detect microcracking or crazing in the resin after each thermal load. Many of the cracks initiated below the sample surface and were detected using transmission optical microscopy. For type I samples, however, scanning electron microscopy was used to detect cracks which occurred on the surface of the specimen. Thermal loads of $\Delta T=220°C$ and below were produced by heating the samples in an oven to the desired temperature difference and then quenching in ice water. Thermal loads of $\Delta T=220°C$ and above were obtained by heating samples in an oven and then quenching in a bath of alcohol and dry ice at -70°C. Both methods produced the same microcracking results for $\Delta T=220°C$. Thermal loads were increased in increments of either 20° or 25°C and no more than one thermal load was applied in any one day to insure that the microcracking was not being produced by thermal fatigue. Between loading times, the specimens were stored in a dry environment so that moisture effects could be discounted.

Microcracking Results and Discussion

Microcracks were observed first in type III samples as shown by the photomicrograph in Fig. 4. The lowest thermal load which produced cracking in these samples was $\Delta T=175°C$ after incrementing the temperature from $\Delta T=150°C$. As seen in Fig. 4, the cracks initiated at the fiber/interphase interface where the fibers are closest together and proceeded radially outward into the coating. Two identical type III specimens showed microcracking in similar locations and directions.

A thermal load of $\Delta T=200°C$ (after incrementing from $\Delta T=175°C$) produced micro-cracking in the type II samples. As shown by the photomicrograph in Fig. 5, the microcracking in this specimen initiated at the coating/matrix interface but did not extend to the fiber surface. The cracks occurred midway between the fibers where the fibers were closest together and radially outward from this location. A totally different mode of cracking was observed in Type I samples for $\Delta T=220°C$ (after incrementing from $\Delta T=200°C$). In this case, microcracking was detected using scanning electron microscopy and is shown in Fig. 6. The interfacial microcrack initiated at the fiber/matrix interface in the hoop direction, at the point where the fibers were nearly touching.

Interphase glass transition had a significant effect on the initiation and location of micro-cracking in the experiments. Microcracking occurred at the lowest thermal loads for the higher T_g interphase (type III). The interphase elastic modulus for this sample type was higher than that of the neat matrix and remained higher throughout most of the thermal cycle. A higher modulus interphase causes an increase in the interfacial thermal stresses which lead to microcracking [33].

Higher thermal loads were required to cause micro-cracking in the type I and type II samples. Type II samples had a lower modulus interphase than the surrounding matrix, particularly at temperatures above the interphase T_g (80°C) and below the matrix T_g (160°C). A lower modulus interphase causes an decrease in the interfacial thermal stresses and increases the resistance to microcracking [33]. Type I samples were particularly resistant to microcracking, behaving again as if a thin, low T_g interphase had formed.

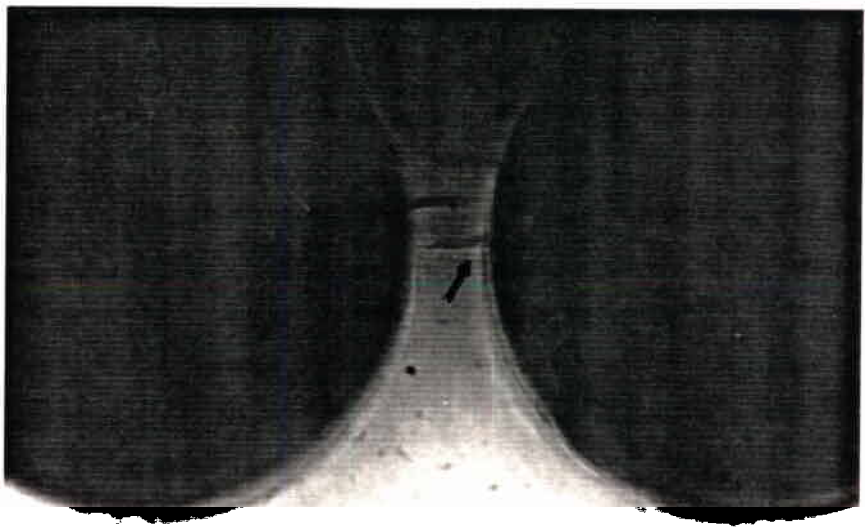

Fig. 4. Photomicrographs of microcracks in specimen type III with EPON 164 coated fibers (625X).

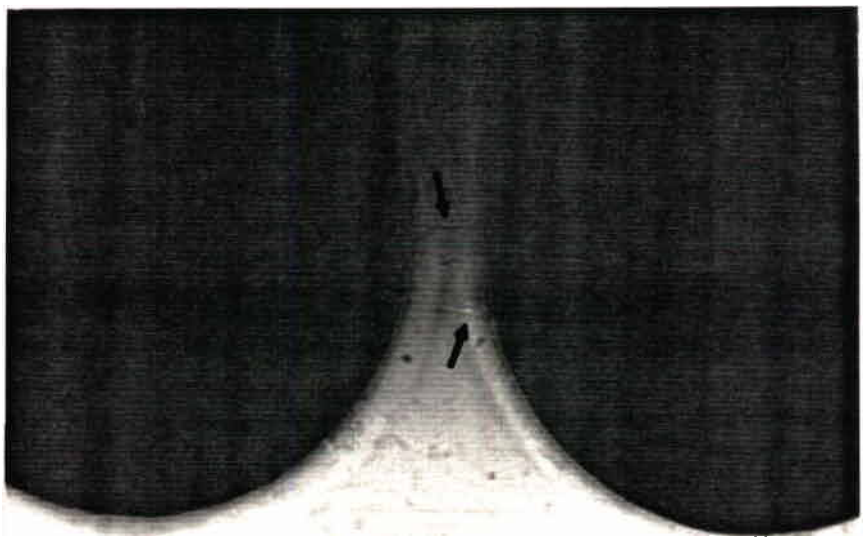

Fig. 5. Photomicrographs of microcracks in specimen type II with EPON 828/871 coated fibers (625X).

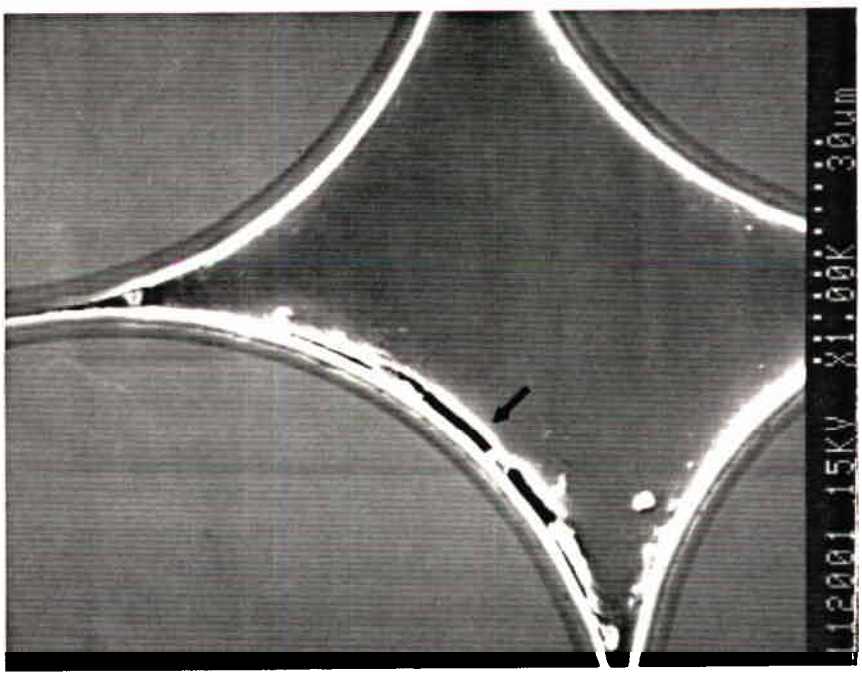

Fig. 6. Photomicrograph of observed failure in specimen I with no fiber coating (1000X).

CONCLUSIONS

Both the interferometric results and the single fiber fragmentation results support the existence of an interphase with reduced glass transition temperature in untreated (type I) samples. As the interphase passed through its glass transition, large changes in surface displacements occurred and interfacial shear strength decreased significantly. Consequently, the ability to transfer load also decreased. These reductions in load transfer occurred at temperatures far below the T_g of the neat matrix. By tailoring the interphase to have a higher T_g, large decreases in interfacial shear strength were avoided.

The properties of the interphase region significantly altered the initiation and location of microcracks in a cluster of fibers. Microcracks occurred at the lowest thermal load in samples with a higher T_g, higher modulus interphase (type III) at the fiber/interphase interface. In samples with a low T_g interphase (type II), microcracks initiated at higher thermal loads and at the interphase/matrix interface. The presence of the low T_g coating prevented cracks from reaching the fiber surface. In samples with no coating (type I), microcracks did not develop until even higher thermal loads and were found to occur in the hoop direction at the fiber surface.

The existence of a reduced T_g has significant implications for the thermal behavior and long term performance of a composite. In the current work, it was shown that interphase glass transition temperature has a significant effect on both load transfer and thermally induced microcracking. Additionally, it was shown that the interphase can be tailored to either enhance or hinder the observed effects.

ACKNOWLEDGMENTS

The authors would like to gratefully acknowledge the support of the Office of Naval Research (Grant # N00014-92-J-1620).

REFERENCES

[1] McCullough, R.L. *Concepts of Fiber-Resin Composites*. Marcel Dekker, Inc., New York, 1971.

[2] Pogony, G.A. *Journal of Materials Science*, Vol. 4, 1969, p. 405.

[3] Lipatov, Y.S., Babich, V.F. and Rosovizky, V.F. *Journal of Applied Polymer Science*, Vol. 20, 1986, p. 1787.

[4] Crowson, R.J. and Arridge, R.G.C. *Journal of Materials Science*, Vol. 12, 1977, p. 2154.

[5] Papanicolaou, G.C. and Theocaris, P.S. *Colloid and Polymer Science*, Vol. 257, 1979, p. 239.

[6] Palmese, G.R. and McCullough, R.L. *Journal of Polymer Science*, Vol. **46**, 1992, p. 1863.

[7] Sottos, N.R., McCullough, R.L. and Scott, W.R., *Composites Science and Technology*, Vol. 44, 1992, p. 319.

[8] Sottos, N.R., Scott, W.R. and McCullough, R.L., *Experimental Mechanics*, Vol. 31, 1991, p. 98.

[9] Sottos, N.R., Ryan, M.J., and Scott, W.R. *Review of Progress in Quantitative Nondestructive Evaluation*, ed by D.O. Thompson and D.E. Chimenti, Plenum Press, New York, Vol. 10A, 1990, p. 1057.

[10] Ryan, M.J., Sottos, N.R. and Scott, W.R. *Review of Progress in Quantitative Nondestructive Evaluation*, ed. by D.O. Thompson and D.E. Chimenti, Plenum Press, New York, Vol. 10B, 1990, p. 2069.

[11] Chamis, C.C. *Composite Materials*, ed. by E.P. Pluddemann, Academic Press, New York, Vol. 6, 1974, p. 32.

[12] Sottos, N.R. *Experiments in Micromechanics of Failure Resistant Materials*, ed. by K.-S. Kim, ASME, New York, AMD-Vol. 130, 1992.

[13] Rao, V. and Drzal, L.T. *Journal of Adhesion*, Vol. 37, 1991, p. 83.

[14] Rao, V. and Drzal, L.T. *Polymer Composites*, Vol. 12, 1991, p. 48.

[15] Wimolkiatisak, A.S. and Bell, J.P. *Polymer Composites*, Vol. 10, 1989, p. 162.

[16] Ohsawa, T., Nakayama, A., Miwa, M. and Hawegawa, A. *Journal of Applied Polymer Science*, Vol. 22, 1978, 3203.

[17] Asloun, E.M., Nardin, M. and Schultz, J. *Journal of Material Science*, 24, 1989, p. 1835.

[18] DiBenedetto, A.T. *Composites Science and Technology*, Vol. 42, 1991, p. 103 .

[19] Theocaris, P.S. and Papanicolaou, G.C. *Fibre Science and Technology*, Vol. 12, 1979, p. 421.

[20] Sottos, N.R. *Polymer Solutions, Blends and Interfaces*, ed. by I. Noda and D.N. Rubingh, Elsevier Science, 1992, p. 339.

[21] Drzal, L.T., Rich, M.J., Camping, J.D. and Park, W.J. Proceedings of the 35th *Annual Technical Conference of the Reinforced Plastics/Composites Institute*, paper 20-C, 1980.

[22] Kelly, A. and Tyson, W.R., *Journal of Mechanics and Physics of Solids*, Vol. 13, 1965, p. 199.

[23] Jayaraman, K. and Reifsnider, K.L. *Proceedings of the Fifth Japan-U.S. Conference on Composite Materials*, Tokyo, Japan, 1990.

[24] Jayaraman, K., Gao, Z. and Reifsnider, K.L. *Proceedings of the Sixth Technical Conference of the American Society for Composites* , 1991.

[25] Uemura, M., Iyama, H. and Yamaguchi, Y. *J. of Thermal Stresses*, Vol. 2, 1979, p. 393.

[26] Nairn, J.A. *Polymer Composites*,. Vol. 6, 1985, 123.

[27] Mikata, Y. and Taya, M. *J. of Composite Materials*, Vol. 19, 1985, 554.

[28] Mikata, Y. and Taya, M. *J. of Applied Mechanics,* Vol. 53, 1986, p. 681.

[29] Pagano, N.J. and Tandon, G.P. *Composites Science and Technology,* Vol. 38, 1990, p. 247.

[30] Sottos, N.R. *The Influence of Interphase Regions on Local Thermal Stresses and Deformations in Composites*, PhD Dissertation, Department of Mechanical Engineering, University of Delaware, 1990.

[31] Sottos, N.R., McCullough, R.L., and Güçeri, S.I. *Mechanics of Composite Structures*, ed. by J.N. Reddy and J.L. Teply, AMD-Vol 100, 1989.

[32] Adams, D.F. J. of Reinforced Plastics and Composites, Vol. 6, 1987, p. 66.

[33] Hiemstra, D.L. and Sottos, N.R. *Journal of Composite Materials*, Vol. 27, No. 10, 1993, p. 1030.